New Journal of Physics
The open access journal at the forefront of physics

Deutsche Physikalische Gesellschaft DPG IOP Institute of Physics

PAPER • OPEN ACCESS

Homogeneous electron liquid in arbitrary dimensions beyond the random phase approximation

To cite this article: L V Duc Pham *et al* 2023 *New J. Phys.* **25** 083040

IOP Publishing New J. Phys. 25 (2023) 083040 https://doi.org/10.1088/1367-2630/acef4c

New Journal of Physics
The open access journal at the forefront of physics

Deutsche Physikalische Gesellschaft DPG
IOP Institute of Physics

Published in partnership with: Deutsche Physikalische Gesellschaft and the Institute of Physics

OPEN ACCESS

RECEIVED
26 April 2023

REVISED
1 August 2023

ACCEPTED FOR PUBLICATION
11 August 2023

PUBLISHED
25 August 2023

PAPER

Homogeneous electron liquid in arbitrary dimensions beyond the random phase approximation

L V Duc Pham[1], **Pascal Sattler**[1], **Miguel A L Marques**[2,*] **and Carlos L Benavides-Riveros**[3,4,*]

[1] Institut für Physik, Martin-Luther-Universität Halle-Wittenberg, 06120 Halle (Saale), Germany
[2] Research Center Future Energy Materials and Systems and Faculty of Mechanical Engineering Chair for Artificial Intelligence for Integrated Materials Science, Ruhr University Bochum, Universitätsstraße 150, D-44801 Bochum, Germany
[3] CNR-INO and Dipartimento di Fisica, Pitaevskii BEC Center, Universitá di Trento, I-38123 Trento, Italy
[4] Max Planck Institute for the Physics of Complex Systems, Nöthnitzer Str. 38, 01187 Dresden, Germany
[*] Authors to whom any correspondence should be addressed.

E-mail: miguel.marques@rub.de and cl.benavidesriveros@unitn.it

Keywords: homogeneous electron gas, electronic correlation, random phase approximation, unconventional dimensions, homogeneous electron liquid, strongly correlated electronic systems

Abstract

The homogeneous electron liquid is a cornerstone in quantum physics and chemistry. It is an archetypal system in the regime of slowly varying densities in which the exchange-correlation energy can be estimated with many methods. For high densities, the behavior of the ground-state energy is well-known for 1, 2, and 3 dimensions. Here, we extend this model to arbitrary integer dimensions and compute its correlation energy beyond the random phase approximation (RPA). We employ the approach developed by Singwi, Tosi, Land, and Sjölander (STLS), whose description of the electronic density response for $2D$ and $3D$ for metallic densities is known to be comparable to Quantum Monte-Carlo. For higher dimensions, we compare the results obtained for the correlation energy with the values previously obtained using RPA. We find that in agreement with what is known for 2 and 3 dimensions, the RPA tends to over-correlate the liquid also at higher dimensions. We furthermore provide new analytical formulae for the unconventional-dimensional case both for the real and imaginary parts of the Lindhard polarizability and for the local field correction of the STLS theory, and illustrate the importance of the plasmon contribution at those high dimensions.

1. Introduction

The ground states of the homogeneous electron gases and liquids have played a prominent role in the modeling and understanding of a wide range of interacting electronic systems [1–14]. They are, in fact, well-known models of choice commonly used to develop, improve and benchmark many approximate approaches for the many-electron problem, including some of the most popular exchange-correlation functionals of density functional theory [15–18].

An important aspect of these systems is the dependency of the correlation energy, among other relevant quantities, on the dimension of the physical space in which they are embedded. This is a quite relevant question in light of the wealth of experimental electronic setups in which one or two of the physical dimensions are much smaller than the remaining ones. As a result, they are usually modeled as one- or two-dimensional quantum systems [19–24]. Furthermore, reduced dimensional systems often exhibit notable physical properties, ranging from Luttinger physics [25] to Moiré superlattices [26]. More recently, progress in the fabrication of artificial materials is paving the way for the realization of non-integer dimensions, as fractal substrates (e.g. Sierpiński carpets of bulk Cu) confining electron gases [27–29]. Quite remarkably, the possibility to circumvent the von Neumann–Wigner theorem, which rules out energy crossings in systems with reduced dimensionality, or to produce unconventional topological phases by engineering (or mimicking) additional synthetic dimensions [30–33] also highlights the importance of

realizing, studying and understanding interacting fermionic systems embedded in non-conventional dimensions.

For the high-density (spin-unpolarized) homogeneous electron gas (HEG) in $D = 1, 2$, and 3 dimensions, the energy per electron can be expanded in terms of r_s, the Wigner-Seitz radius, as follows [34]:

$$\varepsilon_D(r_s \to 0) = \frac{a_D}{r_s^2} - \frac{b_D}{r_s} + c_D \ln r_s + \mathcal{O}(r_s^0)\,. \tag{1}$$

The constants a_D, b_D and c_D are independent of r_s, and their functional form in terms of the dimension D is well known [10]. In recent work, the HEG was extended to arbitrary integer dimensions [35]. It was found a very different behavior for $D > 3$: the leading term of the correlation energy does not depend on the logarithm of r_s, as in equation (1); instead, it scales polynomially as $c_D/r_s^{\eta_D}$, with the exponent $\eta_D = (D-3)/(D-1)$. In the large-D limit, the value of c_D depends linearly on the dimension. This result was obtained within the random-phase approximation (RPA) by summing all the ring diagrams to infinite order.

The RPA is known to be exact in the limit of the dense HEG ($r_s \to 0$), includes long-range interactions automatically, and is applicable to systems where finite-order many-body perturbation theories break down [36]. Yet, unfortunately, it has well-known deficiencies at the metallic (intermediate) densities of the typical homogeneous electron liquid (HEL) (i.e. $1 \leqslant r_s \leqslant 6$). While quantum Monte-Carlo (QMC) is an option [14, 37], there are other high-quality approaches such as the celebrated Singwi, Tosi, Land, and Sjölander (STLS) method that provides results comparable to QMC for those densities regimes [38]. This method attempts to tackle in an approximate manner both the exchange and electronic correlations through a local-field correction. As such, this scheme is often surprisingly accurate in the description of the full electronic density response and is commonly used to investigate quasi-one-dimensional [39], inhomogeneous [40–42] and warm dense electron liquids [43–45]. It has also inspired the development of new functional methods that explicitly retain the dynamical and non-local nature of electronic correlations, while properly accounting for the exchange contribution [46–50]. In sum, while STLS should not be seen as a replacement for QMC methods to obtain accurate correlation energies of the electron liquid, this is a quite insightful (semi-)analytical theory for the many-body physics of this system.

Inspired by the recent theoretical and experimental progress in the dimensional enhancing of many-body systems by mimicking additional synthetic dimensions [51–55], our purpose in this paper is to calculate the correlation energy of the HEL (i.e., the metallic-density regime of the homogeneous electron system) for arbitrary integer dimensions with the STLS method. Our motivation is threefold: first, shed light on the dimensional dependency of electronic properties (as the conductivity or the correlation energy); second, study the performance of the RPA method in the regime of metallic densities for unconventional dimensions; and third, explore the numerical behavior of the STLS method on those dimensions. As expected, one of our main results is that the value of the correlation energy for unconventional dimensions improves significantly with respect to the RPA result (that tends to over-correlate the liquid) obtained previously in [35].

The rest of this paper is organized as follows. In section 2 we review the main STLS equations and rewrite them explicitly in arbitrary D dimensions. We compute the Lindhard polarizability, the structure factor, and the so-called *local field correction* in the Hartree–Fock approximation, providing explicit formulae for some representative systems. In section 3 we explain how the correlation energy is computed in this scheme, and in section 4 discuss the fully polarized case. In sections 5 and 6 we present and discuss our numerical results for the correlation energies as well as the density–density pair distribution function. We also discuss the fulfillment of the compressibility sum rule. In the last section, we present our main conclusions. Three Appendices that give further technical details on our calculations are presented at the end of the paper.

2. STLS theory in D dimensions

In this section, we review the main STLS equations and write them explicitly in arbitrary D dimensions. We follow the standard notation, namely, n is the D-dimensional particle density, Ω is the volume occupied by the electronic liquid, and q_F is the usual Fermi wavevector. We employ atomic units along the paper. To include short-range correlation between electrons, the STLS theory departs from RPA by writing the two-particle density distribution $f_2(\mathbf{r}, \mathbf{p}, \mathbf{r}', \mathbf{p}', t)$ as follows:

$$f_2(\mathbf{r}, \mathbf{p}, \mathbf{r}', \mathbf{p}', t) = f(\mathbf{r}, \mathbf{p}, t) f(\mathbf{r}', \mathbf{p}', t) g_D(\mathbf{r} - \mathbf{r}')\,, \tag{2}$$

where $f(\mathbf{r}, \mathbf{p}, t)$ is the one-particle phase-space density and $g_D(\mathbf{r})$ is the D-dimensional equilibrium, static pair distribution function. Equation (2) can be seen as an ansatz that terminates the hierarchy that otherwise

would write the two-particle distribution function in terms of the three-particle distribution function, and so on. This leads to the following density–density response function [38]:

$$\chi_D(\mathbf{q},\omega) = \frac{\chi_D^0(\mathbf{q},\omega)}{1-\Phi(\mathbf{q})[1-G_D(\mathbf{q})]\chi_D^0(\mathbf{q},\omega)}\,. \tag{3}$$

Here $\chi_D^0(\mathbf{q},\omega)$ is the Lindhard polarizability, i.e. the inhomogeneous non-interacting density response function of an ideal Fermi gas in D dimensions, $G_D(\mathbf{q})$ is the local field correction, and $\Phi(\mathbf{q})$ is the D-dimensional Fourier transform of the Coulomb potential:

$$\Phi(\mathbf{q}) = \frac{(4\pi)^{\frac{D-1}{2}}\Gamma\left(\frac{D-1}{2}\right)}{q^{D-1}}\,, \tag{4}$$

where Γ denotes the gamma function. The presence of $G_D(\mathbf{q})$ in equation (3) is the key feature of the STLS equations that gives the 'beyond RPA' flavor to the theory. This *local field correction* is a direct result of the short-range correlation between the electrons. In arbitrary dimensions, it is given by:

$$G_D(\mathbf{q}) = -\frac{1}{n}\int \mathbf{q}'\cdot\mathbf{q}\frac{q^{D-3}}{q'^{D-1}}\left[S_D(\mathbf{q}-\mathbf{q}')-1\right]\frac{d^D\mathbf{q}'}{(2\pi)^D}\,, \tag{5}$$

with $S_D(\mathbf{q})$ being the structure factor. We can simplify this integral to a two-dimensional one by substituting $\mathbf{q}-\mathbf{q}'=\mathbf{t}$ and using the fact that $S_D(\mathbf{q}) = S_D(q)$ in homogeneous systems. Afterwards, we rewrite the integral using D-dimensional spherical coordinates, where $\mathbf{q}$ is parallel to the Dth-axis, and integrate over all angles except the angle θ between $\mathbf{q}$ and $\mathbf{t}$ to obtain:

$$G_D(\mathbf{q}) = -\frac{q^{D-3}}{(2\pi)^D n}\frac{2\pi^{\frac{D-1}{2}}}{\Gamma\left(\frac{D-1}{2}\right)}\int_0^\infty\int_0^\pi [S_D(t)-1]\frac{[q^2t^{D-1}-qt^D\cos\theta](\sin\theta)^{D-2}}{(q^2+t^2-2qt\cos\theta)^{\frac{D-1}{2}}}d\theta dt\,. \tag{6}$$

Note in passing that in the $2D$ case we must use polar coordinates instead of the spherical coordinates and obtain:

$$G_2(\mathbf{q}) = -\frac{1}{(2\pi)^2 n}\int_0^\infty\int_0^{2\pi}[S_2(t)-1]\frac{qt-t^2\cos\theta}{(q^2+t^2-2qt\cos\theta)^{1/2}}d\theta dt\,. \tag{7}$$

These equations, together with the equation for the dielectric function, $1/\epsilon_D(\mathbf{q},\omega) = 1+\Phi(\mathbf{q})\chi_D(\mathbf{q},\omega)$, lead to an equation for the dielectric function within the STLS theory, namely:

$$\epsilon_D(\mathbf{q},\omega) = 1-\frac{\Phi(\mathbf{q})\chi_D^0(\mathbf{q},\omega)}{1+G_D(\mathbf{q})\Phi(\mathbf{q})\chi_D^0(\mathbf{q},\omega)}\,. \tag{8}$$

Finally, the relation between the structure factor and the dielectric function $\epsilon_D(\mathbf{q},\omega)$ (see, for instance, [56]) can be easily generalized for arbitrary dimensions:

$$S_D(\mathbf{q}) = -\frac{1}{\pi n\Phi(\mathbf{q})}\int_0^\infty \mathrm{Im}\left(\frac{1}{\epsilon_D(\mathbf{q},\omega)}\right)d\omega\,. \tag{9}$$

We can improve the readability of this equation by separating the contributions of the single-particle and plasmon excitations [57]:

$$\begin{aligned} S_D(\mathbf{q}) = &-\frac{1}{\pi n\Phi(\mathbf{q})}\int_0^{qv_F+\frac{q^2}{2}}\mathrm{Im}\left(\frac{1}{\epsilon_D(\mathbf{q},\omega)}\right)d\omega \\ &+\frac{1}{\Phi(\mathbf{q})n}\left(\frac{\partial\mathrm{Re}\epsilon_D(\mathbf{q},\omega)}{\partial\omega}\right)^{-1}\delta(\omega-\omega_p(q))\,, \end{aligned} \tag{10}$$

where v_F is the Fermi velocity and $\omega_p(q)$ is the plasmon dispersion [58]. Equations (6), (8) and (10) form the core of the celebrated STLS set of equations. In this framework, they can be evaluated *self-consistently*. Notice, indeed, that $G_D(\mathbf{q})$ and $S_D(\mathbf{q})$ can be written symbolically as $G_D = \mathcal{F}_1[S_D]$ and $S_D = \mathcal{F}_2[G_D]$, indicating the existence of the mutual functional relations introduced above [49].

We should reiterate here that the crucial aspect of the STLS method is the appearance of the density-density pair distribution function $g_D(\mathbf{r}-\mathbf{r}')$ in the decoupling of the equation of motion (2). Despite the crudeness of such a factorization scheme, the formalism gives correlation energies for both 3D and 2D homogeneous electron gases that significantly improve the RPA results. Unfortunately, the factorization also

results in a number of well-known shortcomings, including negative values of $g_D(\mathbf{r}-\mathbf{r}')$ for sufficiently large values of r_s, and the failure to satisfy the compressibility sum rule (i.e. at long wavelengths the exact screened density response is determined by the isothermal compressibility). The first problem, the un-physical behavior of the pair distribution, is counter-balanced by the fact that the exchange-correlation energy is in reality an integral over $g_D(r)$: it turns out that its value is still quite reasonable in the metallic range as it benefits from an error cancellation [45]. As we will see below, this result, known for the case of 2D and 3D, does also hold for larger dimensions. To tackle the second problem, Vashista and Singwi [59] provided a correction to the STLS method that established the correct compressibility sum rule in the metallic-density regime. This is however a partial solution as both the original STLS method and the Vashista-Singwi extension under-estimate the exchange energy, as pointed out by Sham [60].

2.1. Real part of the Lindhard function for $D = 5, 7$

The expressions for $\chi_2^0(\mathbf{q},\omega)$ and $\chi_3^0(\mathbf{q},\omega)$ are widely known since long ago (see for instance [34, 61]), but higher dimensional expressions are missing in the literature. In appendix A we detail their calculation for higher dimensional settings by performing a linear perturbation from equilibrium. We sketch here the main results.

The real part of $\chi_D^0(\mathbf{q},\omega)$ can be written explicitly as:

$$\begin{aligned}\mathrm{Re}\chi_D^0(\mathbf{q},\omega) = &\frac{2}{(2\pi)^D}\mathcal{P}\int \frac{\Theta(q_F - |\mathbf{p}-\frac{1}{2}\mathbf{q}|)\Theta(|\mathbf{p}+\frac{1}{2}\mathbf{q}|-q_F)}{\omega-\mathbf{p}\cdot\mathbf{q}}d^D\mathbf{p}\\ &-\frac{2}{(2\pi)^D}\mathcal{P}\int \frac{\Theta(|\mathbf{p}-\frac{1}{2}\mathbf{q}|-q_F)\Theta(q_F-|\mathbf{p}+\frac{1}{2}\mathbf{q}|)}{\omega-\mathbf{p}\cdot\mathbf{q}}d^D\mathbf{p},\end{aligned} \tag{11}$$

where $\mathcal{P}$ denotes the principal value. By evaluating these integrals, it is possible to obtain analytical expressions for specific cases. For instance, for $D=5$ and $D=7$ one gets:

$$\begin{aligned}\mathrm{Re}\chi_5^0(\mathbf{q},\omega) = \frac{{q_F}^3}{8\pi^3}\Bigg\{\frac{1}{96\tilde{q}^5}\Bigg[&\left(\frac{3}{2}\left(\tilde{q}^2-2\tilde{\omega}\right)^4+24\tilde{q}^4-12\tilde{q}^2(\tilde{q}^2-2\tilde{\omega})^2\right)\ln\left|\frac{2\tilde{q}-\tilde{q}^2+2\tilde{\omega}}{2\tilde{q}+\tilde{q}^2-2\tilde{\omega}}\right|\\ &+\left(\frac{3}{2}\left(\tilde{q}^2+2\tilde{\omega}\right)^4+24\tilde{q}^4-12\tilde{q}^2(\tilde{q}^2+2\tilde{\omega})^2\right)\ln\left|\frac{2\tilde{q}-\tilde{q}^2-2\tilde{\omega}}{2\tilde{q}+\tilde{q}^2+2\tilde{\omega}}\right|+12\tilde{q}^7-16\tilde{q}^5+144\tilde{q}^3\tilde{\omega}^2\Bigg]-\frac{2}{3}\Bigg\}\end{aligned} \tag{12}$$

and

$$\begin{aligned}\mathrm{Re}\chi_7^0(\mathbf{q},\omega) = \frac{{q_F}^5}{368640\pi^4\tilde{q}^5}\Bigg\{&\left[60(16\tilde{q}^4+3(\tilde{q}^2+2\tilde{\omega})^4-12(\tilde{q}^3+2\tilde{q}\tilde{\omega})^2)-\frac{15(\tilde{q}^2+2\tilde{\omega})^6}{\tilde{q}^2}\right]\ln\left|\frac{2\tilde{q}-\tilde{q}^2-2\tilde{\omega}}{2\tilde{q}+\tilde{q}^2+2\tilde{\omega}}\right|\\ &+\left[60(16\tilde{q}^4+3(\tilde{q}^2-2\tilde{\omega})^4-12(\tilde{q}^3-2\tilde{q}\tilde{\omega})^2)-\frac{15(\tilde{q}^2-2\tilde{\omega})^6}{\tilde{q}^2}\right]\ln\left|\frac{2\tilde{q}-\tilde{q}^2+2\tilde{\omega}}{2\tilde{q}+\tilde{q}^2-2\tilde{\omega}}\right|\\ &-4224\tilde{q}^5+1280\tilde{q}^3(\tilde{q}^4+12\tilde{\omega}^2)-120\tilde{q}(\tilde{q}^8+40\tilde{q}^4\tilde{\omega}^2+80\tilde{\omega}^4)\Bigg\}.\end{aligned} \tag{13}$$

A similar calculation gives a closed expression for the imaginary part:

$$\mathrm{Im}\chi_D^0(\mathbf{q},\omega) = \begin{cases} h(D)\frac{1}{\tilde{q}}\left[\left(1-\nu_-^2\right)^{\frac{D-1}{2}}-\left(1-\nu_+^2\right)^{\frac{D-1}{2}}\right] & \tilde{\omega} < \left|\tilde{q}-\frac{\tilde{q}^2}{2}\right| \text{ and } \tilde{q}<2\\ 0 & \tilde{\omega} < \left|\tilde{q}-\frac{\tilde{q}^2}{2}\right| \text{ and } \tilde{q}>2\\ h(D)\frac{1}{\tilde{q}}\left[1-\nu_-^2\right]^{\frac{D-1}{2}} & \left|\tilde{q}-\frac{\tilde{q}^2}{2}\right| \leqslant \tilde{\omega} \leqslant \tilde{q}+\frac{\tilde{q}^2}{2}\\ 0 & \tilde{\omega} > \tilde{q}+\frac{\tilde{q}^2}{2}\end{cases} \tag{14}$$

where $\tilde{q}=q/q_F$, $\tilde{\omega}=\omega/{q_F}^2$, $h(D)=q_F^{D-2}\left[2^{D-2}(D-1)\pi^{\frac{D-1}{2}}\Gamma\left(\frac{D-1}{2}\right)\right]^{-1}$ and $\nu_\pm=\tilde{\omega}/\tilde{q}\pm\tilde{q}/2$.

2.2. The Hartree–Fock approximation for the first iteration

For the first iteration, the original STLS theory uses the structure factor obtained from the Hartree–Fock calculation [38]. We take the same approach here. Formally, the generalized D-dimensional structure factor is straightforward and reads:

$$S_D^{\mathrm{HF}}(\mathbf{q}) = 1-\frac{2}{(2\pi)^D n}\int_{k,k'\leqslant q_F}\delta(\mathbf{q}-\mathbf{k}'+\mathbf{k})\,d^D\mathbf{k}'d^D\mathbf{k}.$$

Substituting this formal result into equation (5) gives the general D-dimensional expression for the local field correction of STLS within the Hartree–Fock approximation, namely,

$$G_D^{\mathrm{HF}}(\mathbf{q}) = \frac{2q^{D-3}}{(2\pi)^{2D}n^2}\int_{k,k'\leqslant q_F}\frac{\mathbf{q}\cdot(\mathbf{q}+\mathbf{k}-\mathbf{k}')}{|\mathbf{q}+\mathbf{k}-\mathbf{k}'|^{D-1}}\,d^D\mathbf{k}'d^D\mathbf{k}. \tag{15}$$

This integral can be evaluated by making use of the extracule and intracule substitutions: $\mathbf{s} = (\mathbf{k}+\mathbf{k}')/2$and $\mathbf{t} = \mathbf{k}-\mathbf{k}'$. Then, because the integrand only depends on $\mathbf{q}$ and $\mathbf{t}$, one can perform the integration over $\mathbf{s}$. This eventually gives the relevant integration region as the intersection of two hyperspheres, as discussed in detail in appendix B, where we obtain the following expression:

$$\begin{aligned} G_D^{\mathrm{HF}}(\mathbf{q}) = \frac{q^{D-3}}{{q_F}^D\sqrt{\pi}}\frac{\Gamma\left(\frac{D}{2}+1\right)}{\Gamma\left(\frac{D-1}{2}\right)}\int_0^{2q_F}\int_0^{\pi}\mathrm{I}_{1-\frac{t^2}{4{q_F}^2}}\left(\frac{D+1}{2},\frac{1}{2}\right) \\ \times\frac{(q^2+qt\cos\theta)t^{D-1}\sin^{D-2}\theta}{(q^2+t^2+2qt\cos\theta)^{\frac{D-1}{2}}}d\theta dt, \end{aligned} \tag{16}$$

with $I_x(a,b)$ denoting the regularized incomplete beta function. The numerical evaluation of the local field correction as expressed in equation (16) is now a much simpler task. We present the lengthy analytical expression for $G_5^{\mathrm{HF}}(\mathbf{q})$ in appendix B.

3. Energy contributions

The calculation of the kinetic energy of the D-dimensional HEG is as straightforward as it is for $D=3$. It is given by:

$$E_{\mathrm{kin}} = \frac{\alpha_D^2 D}{2(D+2)}\frac{\Upsilon_2(\xi)}{r_s^2}, \tag{17}$$

where $\alpha_D = 2^{(D-1)/D}\Gamma(D/2+1)^{2/D}$,

$$\Upsilon_n(\xi) = \tfrac{1}{2}\left[(1+\xi)^{(D+n)/D}+(1-\xi)^{(D+n)/D}\right]$$

is the spin-scaling function, and ξ is the usual spin-polarization. The interaction energy per particle is given by the following expression:

$$E_{\mathrm{int}} = \frac{1}{\Omega}\sum_{\mathbf{q}\neq 0}\frac{\Phi(\mathbf{q})}{2}(S_D(\mathbf{q})-1). \tag{18}$$

If we introduce the function $\gamma_D(r_s) = -\frac{1}{2q_F}\int_0^{\infty}[S_D(q)-1]dq$ we can rewrite the energy of the unpolarized electron gas in equation (18) as:

$$E_{\mathrm{int}} = -\frac{2^{\frac{D-3}{D}}D^{\frac{2}{D}}}{\sqrt{\pi}}\Gamma\left(\frac{D-1}{2}\right)\Gamma\left(\frac{D}{2}\right)^{\frac{2-D}{D}}\frac{\gamma_D(r_s)}{r_s}.$$

By using the adiabatic-connection formula, the total interaction energy per particle can be computed by using the formula [62]: $\int_0^1\lambda E_{\mathrm{int}}(\lambda r_s)d\lambda$, where λ is a coupling constant that represents the strength of the interaction. Therefore, the full ground-state energy of the unpolarized electron gas in the STLS theory can then be written as:

$$E_0 = \frac{\alpha_D^2 D}{2(D+2)}\frac{\Upsilon_2(0)}{r_s^2} - E(D)\frac{1}{r_s^2}\int_0^{r_s}\gamma_D(r_s')dr_s', \tag{19}$$

where $E(D)$ is defined as:

$$E(D) = \frac{2^{\frac{D-3}{D}}D^{\frac{2}{D}}}{\sqrt{\pi}}\Gamma\left(\frac{D-1}{2}\right)\Gamma\left(\frac{D}{2}\right)^{\frac{2-D}{D}}. \tag{20}$$

To obtain the correlation energy we need to make use of the Hartree–Fock energy. While the kinetic energy is already calculated, the calculation of the exchange energy is not trivial. This was already calculated by two of us in [35]:

$$E_{\mathrm{HF}} = \frac{\alpha_D^2 D}{2(D+2)}\frac{\Upsilon_2(\xi)}{r_s^2} - \frac{2\alpha_D D}{\pi(D^2-1)}\frac{\Upsilon_1(\xi)}{r_s}. \tag{21}$$

Since the correlation energy is defined as the difference between the ground-state energy and the ground-state Hartree–Fock energy, we get for the D-dimensional gas the following compact formula:

$$E_{\rm corr} = \frac{1}{r_s^2}\int_0^{r_s}\left[-E(D)\gamma_D(r_s') + \frac{2\alpha_D D\Upsilon_1(0)}{\pi\,(D^2-1)}\right]dr_s'\,. \tag{22}$$

This is the formula we are going to use for the calculation of the correlation energy.

4. The fully polarized case

The extension of the above equations for the fully polarized case is quite straightforward (for $D=3$ see [63, 64]). The relation between the local field correction and the structure factor is given by:

$$G_D^{\uparrow\uparrow}(q) = -\frac{1}{n}\int\frac{(\mathbf{q}'\cdot\mathbf{q})q^{D-3}}{q'^{D-1}}[S_D^{\uparrow\uparrow}(\mathbf{q}-\mathbf{q}')-1]\frac{d^D\mathbf{q}'}{(2\pi)^D}\,, \tag{23}$$

where $S_D^{\uparrow\uparrow}(\mathbf{q}-\mathbf{q}')$ is the spin-resolved structure factor. The corresponding density-density response function is given by:

$$\chi_D^{\uparrow\uparrow}(\mathbf{q},\omega) = \frac{\chi_D^{0,\uparrow\uparrow}(\mathbf{q},\omega)}{1-\Phi(\mathbf{q})[1-G_D^{\uparrow\uparrow}(\mathbf{q})]\chi_D^{0,\uparrow\uparrow}(\mathbf{q},\omega)}\,. \tag{24}$$

where $\chi_D^{0,\uparrow\uparrow}(\mathbf{q},\omega)$ is the polarizability of the fully polarized non-interacting HEG that can be easily related with the spinless quantities $\chi_D^0(\mathbf{q},\omega)$ by a factor of $1/2$ [34]. In addition, the Fermi wavevector should be re-scaled $q_{F,\uparrow} = 2^{1/D}q_F$. Finally, the fluctuation-dissipation theorem leads to:

$$S_D^{\uparrow\uparrow}(\mathbf{q}) = -\frac{1}{\pi\,n}\int_0^\infty {\rm Im}\chi_D^{\uparrow\uparrow}(\mathbf{q},\omega)d\omega\,. \tag{25}$$

As a result, in the fully polarized case, the correlation energy is given by:

$$E_{\rm corr} = \frac{1}{r_s^2}\int_0^{r_s}\left[-F(D)\gamma_D^{\uparrow\uparrow}(r_s') + \frac{2\alpha_D D\Upsilon_1(1)}{\pi\,(D^2-1)}\right]dr_s'\,. \tag{26}$$

where $F(D)$ is a simple re-scaling of $E(D)$ in equation (20):

$$F(D) = 2^{1/D}E(D)\,, \tag{27}$$

and $\gamma_D^{\uparrow\uparrow}(r_s) = -\frac{1}{2q_{F,\uparrow}}\int_0^\infty[S_D^{\uparrow\uparrow}(q)-1]dq$.

5. Numerical results

Starting from the expression for the local field correction in the Hartree–Fock approximation $G_D^{\rm HF}(\mathbf{q})$ presented in section 2.2 we calculated $S_D(\mathbf{q})$ using equation (10). In this case $\omega_p(q)$ is obtained from the zero of the dielectric function $\epsilon_D(\mathbf{q},\omega)$, which in turn is given by equation (8). We then started the entire self-consistent cycle of the STLS equations. To improve the convergence of the iterative procedure we applied the following linear mixing:

$$\bar{G}_D^i(\mathbf{q}) = G_D^{i-1}(\mathbf{q}) + [G_D^i(\mathbf{q}) - G_D^{i-1}(\mathbf{q})]/a\,, \tag{28}$$

where i is the iteration number and a takes values between 1 and 3.5 (for the 5D and the 7D cases we used $a=1.5$). At each iteration, we calculated the quantity $\gamma_D(r_s)$ with the new structure factor $S_D(\mathbf{q})$. After 10 iterations we obtained convergence in $\gamma_D(r_s)$ within 0.1%. The value of $\gamma_D(r_s)$ at the end of the self-consistent calculation is then used to calculate the correlation energy using equation (22).

We first benchmarked our implementation for 2D and 3D. The results are presented in figure 1, where it can be seen that we recovered the original STLS results and obtained the well-known agreement of STLS with the Quantum Monte-Carlo results [65, 66]. In the 2D case we also obtained similar results to the ones obtained previously by Jonson [67]. The decrease of the magnitude of the correlation energy in the paramagnetic case is consistent with the Quantum Monte-Carlo results [14].

Our new results for the HEL in 5D and 7D (for which we were able to compute analytically the Lindhard polarizability and the local field correction) in the paramagnetic and the ferromagnetic case are presented in

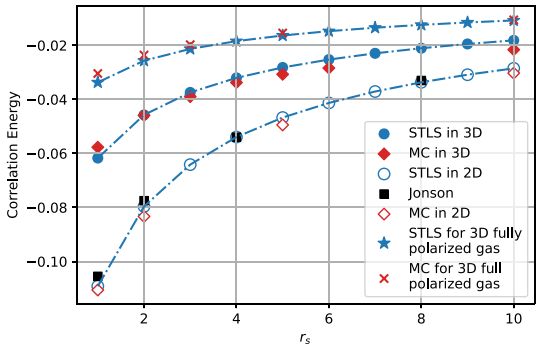

Figure 1. Correlation energy for HEL in 3*D* and 2*D* expressed as a function of r_s. Our results for STLS in the paramagnetic case are compared with the results of Jonson [67] and the results of QMC from [65, 66]. In the ferromagnetic case our results for STLS are compared with the results of QMC from [14].

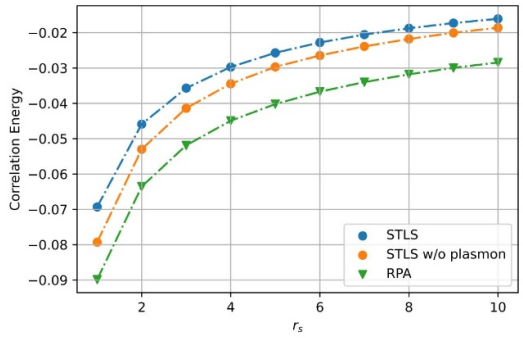

(a) HEL in 5D

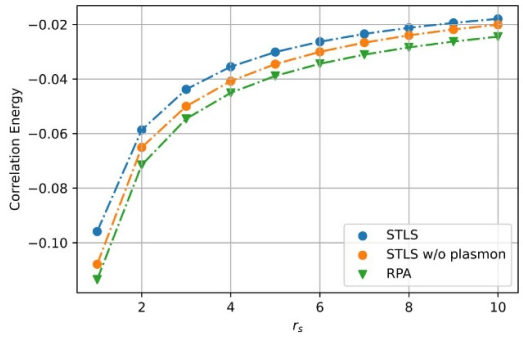

(b) HEL in 7D

Figure 2. Correlation energy of the unpolarized HEL in 5*D* and 7*D* expressed as a function of r_s. Our results for STLS with and without the plasmon contribution are compared with RPA results from [35].

figures 2(a), (b) and 3(a), (b), respectively. Those are compared with the RPA results previously obtained in [35, 68]. It is a general result of our implementation that the STLS correlation energy decreases (in absolute value) in comparison with the one from RPA, which confirms that this latter approximation tends to over-correlate the gas, even in dimensions higher than 3. Yet, for high dimensions, the general error of RPA is smaller, both in the ferromagnetic and the paramagnetic cases. The correlation energy is smaller in magnitude in the ferromagnetic case in comparison with the paramagnetic one in all the dimensions studied, the same behavior found with the RPA. Furthermore, since the structure factor of STLS can be easily separated into the pair and the plasmonic contributions [56, 58], we investigated the plasmon contribution separately by calculating the correlation energy with and without it. We conclude that the plasmonic correction is more relevant for intermediate densities at all dimensions: this term indeed improves the correlation energy on average by 30.9% in the 5D case and 49.2% in the 7D case.

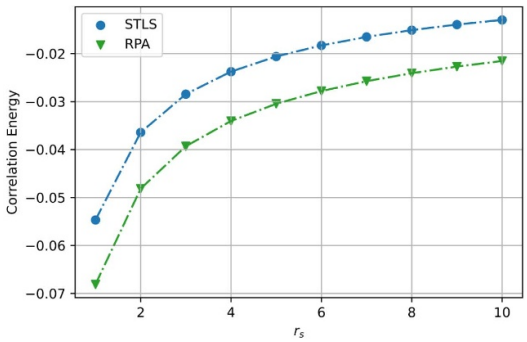

(a) HEL in 5D

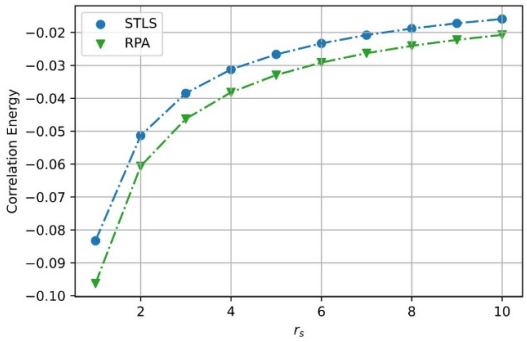

(b) HEL in 7D

Figure 3. Correlation energy of the fully polarized HEL in 5*D* and 7*D* expressed as a function of r_s. Our results for STLS are compared with the RPA results from [35].

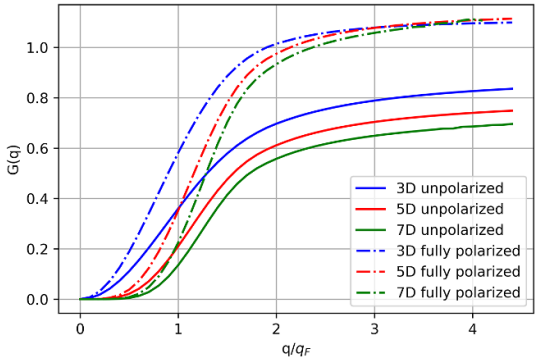

Figure 4. The local field correction $G_D(\mathbf{q})$ for $r_s = 2$ in the 3*D*, 5*D* and 7*D* case for the para- and ferromagnetic HEL.

For the sake of completeness, we also present in figure 4 the values for the local field correction $G_D(\mathbf{q})$ we obtained for both paramagnetic and ferromagnetic gases for $D = 3, 5, 7$ for a selected value of the density (i.e. $r_s = 2$). While the magnitude of the local correction is larger for the fully polarized gas, the global value diminishes for large dimensions in the whole domain of q.

Finally, to study the quality of the density-density pair distribution function $g_D(r)$ we compute it by utilizing the fact that $g_D(r) - 1$ is the Fourier transform of $(1/n)[S_D(q) - 1]$ and plot $g_D(r)$ as well as $S_D(q)$ at the metallic density $r_s = 5$ and the large radius $r_s = 10$ for dimensions $D = 3, 5$, and 7 (see figures 5 and 6). The behavior of $g_D(r)$ for the metallic densities (i.e. $r_s = 5$) is physical in the sense that it takes positive values for all the analyzed dimensions, whereas for $r_s = 10$ an un-physical, though small, negative value can be observed for small distances. This is in agreement with the 2D and 3D cases, discussed above; this also shows that the range of validity of the STLS scheme is limited to the metallic-density regime, even at unconventional dimensions.

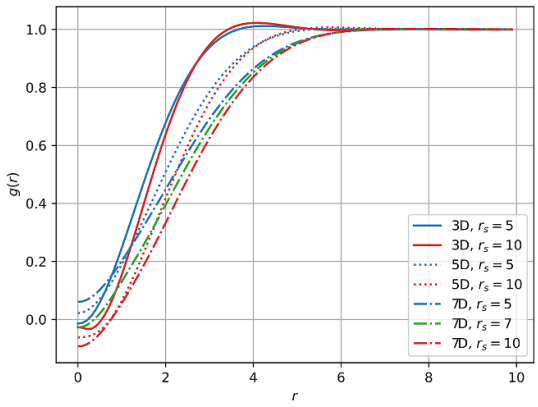

Figure 5. The density-density pair distribution $g_D(r)$ of the HEL is sketched at $r_s = 5$ and 10 for dimensions $D = 3, 5$ and 7.

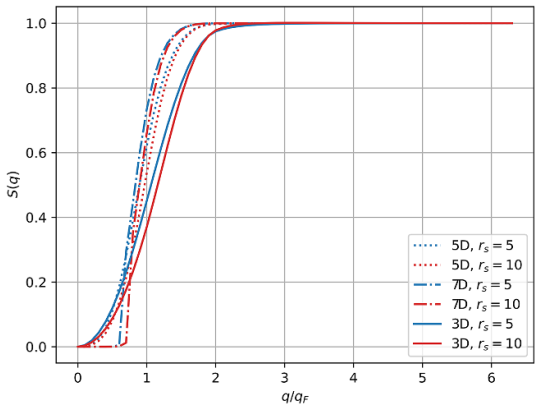

Figure 6. The structure factor $S_D(q)$ at $r_s = 5$ and 10 for dimensions $D = 3, 5$ and 7.

6. Sum rules

As already mentioned, one of the known shortcomings of the STLS method is the failure to satisfy the compressibility sum rule (CSR) which is an exact property of the HEL. In the long wavelength limit, the static response and dielectric functions are related to the compressibility of the electronic system. For arbitrary dimensions, the following exact expression holds (see appendix C):

$$\lim_{q\to 0} \epsilon_D(\mathbf{q}, 0) = 1 + \left(\frac{q_{\mathrm{TF}}}{q}\right)^{D-1} \frac{\kappa}{\kappa_f}, \tag{29}$$

where κ/κ_f is the ratio of the compressibility of the interacting-free D-dimensional electron liquid, and q_{TF} is the D-dimensional Thomas-Fermi wave vector. For the free electron liquid, the corresponding free compressibility is $\kappa_f = Dr_s^2/n\alpha_D^2$. Also by taking the limit $q \to 0$ at $\omega = 0$ in equation (8) and comparing the result with equation (29) (see also appendix C) one obtains:

$$\frac{\kappa_f}{\kappa} = 1 - \gamma_D \left(\frac{q_{\mathrm{TF}}}{q_F}\right)^{D-1} \equiv \mathcal{K}_D\,. \tag{30}$$

Another way to calculate the same compressibility ratio in arbitrary dimensions is to use both the thermodynamic formula $\kappa^{-1} = n(\partial P/\partial n)$, where P denotes the pressure, and the expression of the energy for the free liquid (17), which leads to

$$\frac{\kappa_f}{\kappa} = \frac{r_s^4}{\alpha_D^2 D}\left[\frac{(1-D)}{r_s}\epsilon_D'(r_s) + \epsilon_D''(r_s)\right] \equiv \bar{\mathcal{K}}_D\,. \tag{31}$$

In practice, equation (29) implies that the compressibility ratio κ/κ_f derived from the thermodynamic expression in equation (31) should be equal to the same ratio derived from the $\lim_{q\to 0}\epsilon_D(\mathbf{q}, 0)$ of

Table 1. Compressibility ratios $\mathcal{K}_D$ (30) and $\bar{\mathcal{K}}_D$ (31) predicted by the STLS scheme in 3*D*, 5*D* and 7*D*.

	3*D*		5*D*		7*D*	
	$\mathcal{K}_3$	$\bar{\mathcal{K}}_3$	$\mathcal{K}_5$	$\bar{\mathcal{K}}_5$	$\mathcal{K}_7$	$\bar{\mathcal{K}}_7$
$r_s = 2$	0.35	0.64	0.75	0.88	0.85	0.93
$r_s = 4$	−0.39	0.25	0.46	0.73	0.69	0.85
$r_s = 6$	−1.18	−0.16	0.15	0.58	0.52	0.77

equation (8) with $G_D(\mathbf{q})$ as given in equation (6). Yet, calculating the compressibility from an approximate expression of the dielectric function will generally result in a value that differs from the one obtained as the derivative of the pressure. This is the case of STLS theory, indeed. As a matter of fact, there are few theoretical settings where they coincide [69].

The numerical results of κ_f/κ in 3*D*, 5*D* and 7*D* calculated both as $\mathcal{K}_D$ (30) and $\bar{\mathcal{K}}_D$ (31) for some r_s are shown in table 1. In general, for all dimensions $\mathcal{K}_D \neq \bar{\mathcal{K}}_D$. For 3D we obtained the results of the original STLS paper [38]. Notice that the STLS compressibility ratio $\mathcal{K}_3$ becomes already negative for $r_s > 3$. Yet, interestingly, the larger the underlying dimension the better the performance of the CSR within the original STLS framework. For instance, for $r_s = 4$, $\mathcal{K}_D/\bar{\mathcal{K}}_D = -1.56, 0.63$, and 0.81 for 3*D*, 5*D* and 7*D*, respectively.

There are other well-known sum rules that can be discussed in the context of STLS [70]. For instance, in the limit of large frequencies, one can show that $\epsilon_D(\mathbf{q},\omega) = 1 - [\omega'_D(\mathbf{q})/\omega]^2$, where $[\omega'_D(\mathbf{q})]^2 = \Phi(\mathbf{q})nq^2$ is a frequency that in the case of $D = 3$ is equal to $\omega_p^2 = 4\pi n$, the plasma frequency of the liquid. Moreover, by using the results of appendix C and the frequency moment sum rules [70], it is also straightforward to see that the so-called screening requirement is independent of the dimension of the space:

$$\lim_{q\to 0}[\epsilon_D(\mathbf{q},0)]^{-1} = 0\,. \tag{32}$$

7. Conclusion and outlook

In this paper, we have studied the homogeneous electron liquid (HEL) in arbitrary integer dimensions beyond the random phase approximation (RPA). Our main motivation was to study the quality of the RPA results previously obtained for the homogeneous electron gas in dimensions larger than 3 [35]. To that goal, we have employed the Singwi, Tosi, Land, and Sjölander (STLS) scheme whose accuracy to compute the full electronic density response is comparable to Quantum Monte-Carlo. We provided new analytical formulae for the real and imaginary parts of the Lindhard polarizability and for the so-called local field correction of the STLS theory. We have also discussed the un-physical predictions of the STLS method for large values of r_s in arbitrary dimensions and the incapability of the scheme of fulfilling the compressibility sum rule. From our results, we can conclude that the algebraic properties of the correlation energy found in [35] are mainly valid in the high-density limit of the homogeneous electron gas. Furthermore, in agreement with what is known for 2 and 3 dimensions, the RPA tends to over-correlate the gas, also in the high dimensions studied here. This result can potentially shed light on the more far-reaching problems of quantum many-body systems embedded in fractional or synthetic dimensions [27, 29, 71–73]. We believe that the results of this paper can be a useful framework to improve our overall comprehension of Coulomb gases, and to develop a more coherent and unified dimensional approach to the correlation problem of those systems [22, 74–76].

Data availability statement

All data that support the findings of this study are included within the article (and any supplementary files).

Acknowledgments

We thank Robert Schlesier for helpful discussions. We acknowledge financial support from 'BiGmax', the Max Planck Society's research network on big-data-driven materials science, and the European Union's Horizon Europe Research and Innovation program under the Marie Skłodowska-Curie Grant Agreement No 101065295 (C.L.B.-R.).

Appendix A. Calculation of the Lindhard polarizability in $D \geqslant 3$

To compute the Lindhard polarizability for dimensions larger than 3 we start by writing the one-particle density and the external potential as linear perturbations from equilibrium:

$$\begin{aligned} f(\mathbf{r},\mathbf{p},t) &= f_0(\mathbf{p}) + \lambda\,\delta f(\mathbf{r},\mathbf{p},t)\,, \\ v(\mathbf{r},t) &= v_0(\mathbf{r}) + \lambda\,\delta v(\mathbf{r},t)\,. \end{aligned} \tag{A1}$$

After substituting equation (A1) in equation (2) one obtains the following result for the induced charge density $\rho_{\mathrm{ind}}(\mathbf{q},\omega)$:

$$\rho_{\mathrm{ind}}(\mathbf{q},\omega) = \frac{\chi_D^0(\mathbf{q},\omega)}{1-\Phi(\mathbf{q})[1-G_D(\mathbf{q})]\chi^0(\mathbf{q},\omega)}\delta v(\mathbf{q},\omega)\,, \tag{A2}$$

where $\chi_D^0(\mathbf{q},\omega)$ is given by:

$$\chi_D^0(\mathbf{q},\omega) = -\lim_{\eta\to 0^+}\int \frac{\mathbf{q}\cdot\nabla_{\mathbf{p}} f_0(\mathbf{p})}{\omega + i\eta - \mathbf{p}\cdot\mathbf{q}}d^D\mathbf{p} \tag{A3}$$

By using the Taylor expansion: $f_0(\mathbf{p}\pm\frac{1}{2}\mathbf{q}) = f_0(\mathbf{p}) \pm \frac{1}{2}\mathbf{q}\cdot\nabla_{\mathbf{p}} f_0(\mathbf{p}) + \cdots$, we can then rewrite $\chi_D^0(\mathbf{q},\omega)$ as:

$$\chi_D^0(\mathbf{q},\omega) \approx \lim_{\eta\to 0^+}\int \frac{f_0(\mathbf{p}-\frac{1}{2}\mathbf{q}) - f_0(\mathbf{p}+\frac{1}{2}\mathbf{q})}{\omega + i\eta - \mathbf{p}\cdot\mathbf{q}}d^D\mathbf{p}\,. \tag{A4}$$

This is the Lindhard polarizability of a D-dimensional Fermi gas [77].

At $T=0$ the equilibrium density reads

$$f_0(\mathbf{p}\pm\tfrac{1}{2}\mathbf{q}) = \frac{2}{(2\pi)^D}\Theta\left[\tfrac{1}{2}\left({q_F}^2 - \left|\mathbf{p}\pm\tfrac{1}{2}\mathbf{q}\right|^2\right)\right] = \frac{2}{(2\pi)^D}\Theta(q_F - |\mathbf{p}\pm\tfrac{1}{2}\mathbf{q}|)\,. \tag{A5}$$

Plugging these equations and the identity $\lim_{\eta\to 0^+}\frac{1}{x-x_0\pm i\eta} = \mathcal{P}\frac{1}{x-x_0} \mp i\pi\,\delta(x-x_0)$ into equation (A4) yields:

$$\begin{aligned} \chi_D^0(\mathbf{q},\omega) = {}& \frac{2}{(2\pi)^D}\mathcal{P}\int \frac{\Theta(q_F - |\mathbf{p}-\frac{1}{2}\mathbf{q}|) - \Theta(q_F - |\mathbf{p}+\frac{1}{2}\mathbf{q}|)}{\omega - \mathbf{p}\cdot\mathbf{q}}d^D\mathbf{p} \\ & - i\frac{2\pi}{(2\pi)^D}\int\left[\Theta\left(q_F - \left|\mathbf{p}-\frac{1}{2}\mathbf{q}\right|\right) - \Theta\left(q_F - \left|\mathbf{p}+\frac{1}{2}\mathbf{q}\right|\right)\right]\delta(\omega - \mathbf{p}\cdot\mathbf{q})\,d^D\mathbf{p}\,. \end{aligned} \tag{A6}$$

The real part of $\chi_D^0(\mathbf{q},\omega)$ can then be rewritten as:

$$\begin{aligned} \mathrm{Re}\chi_D^0(\mathbf{q},\omega) = {}& \frac{2}{(2\pi)^D}\mathcal{P}\int \frac{\Theta(q_F - |\mathbf{p}-\frac{1}{2}\mathbf{q}|)\Theta(|\mathbf{p}+\frac{1}{2}\mathbf{q}| - q_F)}{\omega - \mathbf{p}\cdot\mathbf{q}}d^D\mathbf{p} \\ & - \frac{2}{(2\pi)^D}\mathcal{P}\int \frac{\Theta(|\mathbf{p}-\frac{1}{2}\mathbf{q}| - q_F)\Theta(q_F - |\mathbf{p}+\frac{1}{2}\mathbf{q}|)}{\omega - \mathbf{p}\cdot\mathbf{q}}d^D\mathbf{p}\,. \end{aligned} \tag{A7}$$

The second integral can be rewritten with the substitution $\mathbf{p}\to-\mathbf{p}$ so that the expression of $\mathrm{Re}\chi_D^0(\mathbf{q},\omega)$ reduces to just one single integral:

$$\mathrm{Re}\chi_D^0(\mathbf{q},\omega) = \frac{2}{(2\pi)^D}\mathcal{P}\int \Theta(q_F - |\mathbf{p}-\tfrac{1}{2}\mathbf{q}|)\Theta(|\mathbf{p}+\tfrac{1}{2}\mathbf{q}| - q_F)\left(\frac{1}{\omega - \mathbf{p}\cdot\mathbf{q}} - \frac{1}{\omega + \mathbf{p}\cdot\mathbf{q}}\right)d^D\mathbf{p}\,. \tag{A8}$$

Utilizing the following property of the Heaviside step function: $\Theta(x) = 1 - \Theta(-x)$ and the symmetry of the integrand under the transformation $\mathbf{p}\to-\mathbf{p}$, $\mathrm{Re}\chi^0(\mathbf{q},\omega)$ can be further simplified to:

$$\mathrm{Re}\chi_D^0(\mathbf{q},\omega) = \frac{2}{(2\pi)^D}\mathcal{P}\int \Theta(q_F - |\mathbf{p}-\tfrac{1}{2}\mathbf{q}|)\left(\frac{1}{\omega - \mathbf{p}\cdot\mathbf{q}} - \frac{1}{\omega + \mathbf{p}\cdot\mathbf{q}}\right)d^D\mathbf{p}\,. \tag{A9}$$

This integral becomes dimensionless by putting $\mathbf{p} - \frac{\mathbf{q}}{2} = \mathbf{k}$ and introducing the following substitutions $\tilde{\mathbf{q}} = \mathbf{q}/q_F$, $\tilde{\mathbf{k}} = \mathbf{k}/q_F$ and $\tilde{\omega} = \omega/{q_F}^2$:

$$\mathrm{Re}\chi_D^0(\mathbf{q},\omega) = \frac{2q_F^{D-2}}{(2\pi)^D}\mathcal{P}\int \Theta(1-\tilde{k})\left(\frac{1}{\tilde{\omega} - \tilde{\mathbf{q}}\cdot\tilde{\mathbf{k}} - \frac{\tilde{q}^2}{2}} - \frac{1}{\tilde{\omega} + \tilde{\mathbf{q}}\cdot\tilde{\mathbf{k}} + \frac{\tilde{q}^2}{2}}\right)d^D\tilde{\mathbf{k}}\,. \tag{A10}$$

To solve this integral we choose D-dimensional spherical coordinates such that $\tilde{\mathbf{q}}$ is parallel to the last axis:

$$\mathrm{Re}\chi_D^0(\mathbf{q},\omega) = \frac{2q_F^{D-2}}{(2\pi)^D}\frac{2\pi^{\frac{D-1}{2}}}{\Gamma\left(\frac{D-1}{2}\right)}\mathcal{P}\int_0^1\int_0^\pi\left(\frac{\tilde{k}^{D-1}\sin^{D-2}\theta}{\tilde{\omega}-\tilde{q}\tilde{k}\cos\theta-\frac{\tilde{q}^2}{2}}-\frac{\tilde{k}^{D-1}\sin^{D-2}\theta}{\tilde{\omega}+\tilde{q}\tilde{k}\cos\theta+\frac{\tilde{q}^2}{2}}\right)d\theta d\tilde{k}, \tag{A11}$$

where θ is the angle between $\tilde{\mathbf{q}}$ and $\tilde{\mathbf{k}}$. The full evaluation of this integral is quite involved. We just mention that this gives the known result for $D=3$:

$$\begin{aligned}\mathrm{Re}\chi_3^0(\mathbf{q},\omega) = \frac{q_F}{2\pi^2}\Bigg\{&-1+\frac{1}{2\tilde{q}}\left[1-\left(\frac{2\tilde{\omega}-\tilde{q}^2}{2\tilde{q}}\right)^2\right]\ln\left|\frac{2\tilde{q}-\tilde{q}^2+2\tilde{\omega}}{2\tilde{q}+\tilde{q}^2-2\tilde{\omega}}\right|\\&-\frac{1}{2\tilde{q}}\left[1-\left(\frac{2\tilde{\omega}+\tilde{q}^2}{2\tilde{q}}\right)^2\right]\ln\left|\frac{2\tilde{q}+\tilde{q}^2+2\tilde{\omega}}{2\tilde{q}-\tilde{q}^2-2\tilde{\omega}}\right|\Bigg\}.\end{aligned} \tag{A12}$$

We provide the explicit results for $D=5$ in (12) and $D=7$ in (13).

The imaginary part of the Lindhard polarizability can be computed by using the same substitutions as in the calculation of $\mathrm{Re}\chi_D^0(\mathbf{q},\omega)$:

$$\mathrm{Im}\chi_D^0(\mathbf{q},\omega) = -\frac{q_F^{D-2}}{(2\pi)^{D-1}}\int[\Theta(1-\tilde{k})-\Theta(1-|\tilde{\mathbf{q}}+\tilde{\mathbf{k}}|)]\delta\left(\tilde{\omega}-\tilde{\mathbf{q}}\cdot\tilde{\mathbf{k}}-\frac{\tilde{q}^2}{2}\right)d^D\tilde{\mathbf{k}}. \tag{A13}$$

Next we want to investigate the symmetry of $\mathrm{Im}\chi_D^0(\mathbf{q},\omega)$. By considering $\mathrm{Im}\chi_D^0(-\mathbf{q},-\omega)$ and substituting $\tilde{\mathbf{k}}'=\tilde{\mathbf{k}}-\tilde{\mathbf{q}}$ we realize that $\mathrm{Im}\chi_D^0(\mathbf{q},\omega) = -\mathrm{Im}\chi_D^0(-\mathbf{q},-\omega)$. This symmetry allows us to restrict ourselves to case where $\omega>0$. $\mathrm{Im}\chi_D^0(\mathbf{q},\omega)$ can then be rewritten for positive ω as follows:

$$\mathrm{Im}\chi_D^0(\mathbf{q},\omega) = -\frac{q_F^{D-2}}{(2\pi)^{D-1}}\int\Theta(1-\tilde{k})\Theta(|\tilde{\mathbf{q}}+\tilde{\mathbf{k}}|-1)\delta\left(\tilde{\omega}-\tilde{\mathbf{q}}\cdot\tilde{\mathbf{k}}-\frac{\tilde{q}^2}{2}\right)d^D\tilde{\mathbf{k}}. \tag{A14}$$

There are 2 cases where the integrand is different from 0:

- $\left|\tilde{q}-\frac{\tilde{q}^2}{2}\right| \leqslant \tilde{\omega} \leqslant \tilde{q}+\frac{\tilde{q}^2}{2}$
- $\tilde{\omega} < \tilde{q}-\frac{\tilde{q}^2}{2}$, $\tilde{q}<2$

The evaluation of both integrals is technically similar. Thus we just want to discuss the evaluation in the first case. The minimum value of $\tilde{k}$ in the first case is $\tilde{k}_{\min} = |\tilde{\omega}/\tilde{q}-\tilde{q}/2|$. Performing the integration over all angles except the angle θ between $\tilde{\mathbf{q}}$ and $\tilde{\mathbf{k}}$ and substituting $\cos\theta = t$ leads to:

$$\mathrm{Im}\chi_D^0(\mathbf{q},\omega) = -\frac{q_F^{D-2}}{(2\pi)^{D-1}}\frac{2\pi^{\frac{D-1}{2}}}{\Gamma\left(\frac{D-1}{2}\right)}\frac{1}{\tilde{q}}\int_{\left|\frac{\tilde{\omega}}{\tilde{q}}-\frac{\tilde{q}}{2}\right|}^1\int_{-1}^1\delta\left(\frac{\tilde{\omega}}{\tilde{q}\tilde{k}}-\frac{\tilde{q}}{2\tilde{k}}-t\right)\tilde{k}^{D-2}(1-t^2)^{\frac{D-3}{2}}dtd\tilde{k}. \tag{A15}$$

To evaluate it we should put $\tilde{\omega} = \tilde{q}^2/2+\tilde{q}\tilde{k}\cos\theta \Rightarrow -1 \leqslant \tilde{\omega}/\tilde{q}\tilde{k}-\tilde{q}/2\tilde{k} \leqslant 1$, so that the integral over t can be carried out easily. We obtain in this case the following result:

$$\mathrm{Im}\chi_D^0(\mathbf{q},\omega) = h(D)\frac{1}{\tilde{q}}\left[1-\nu_-^2\right]^{\frac{D-1}{2}}, \tag{A16}$$

where we define $h(D) = q_F^{D-2}\left[2^{D-2}(D-1)\pi^{\frac{D-1}{2}}\Gamma\left(\frac{D-1}{2}\right)\right]^{-1}$ and $\nu_\pm = \tilde{\omega}/\tilde{q}\pm\tilde{q}/2$.

In the second case, $k_{\min} = \sqrt{1-2\omega}$ and we obtain the following result:

$$\mathrm{Im}\chi_D^0(\mathbf{q},\omega) = h(D)\frac{1}{\tilde{q}}\left[\left(1-\nu_-^2\right)^{\frac{D-1}{2}}-\left(1-\nu_+^2\right)^{\frac{D-1}{2}}\right]. \tag{A17}$$

Eventually $\mathrm{Im}\chi_D^0(\mathbf{q},\omega)$ reads as in equation (14).

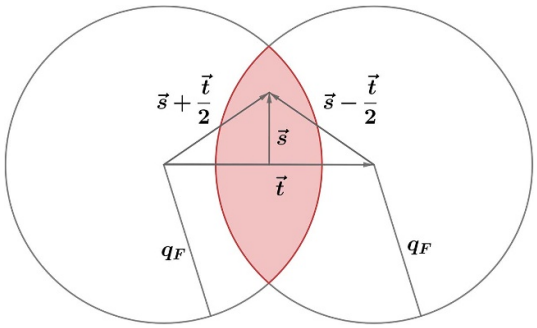

Figure 7. Integration region of $G_D^{\mathrm{HF}}(\mathbf{q})$.

Appendix B. The local field correction in the Hartree–Fock approximation

After the substitution $\mathbf{s} = (\mathbf{k}+\mathbf{k}')/2$and $\mathbf{t} = \mathbf{k}-\mathbf{k}'$ equation (15) becomes:

$$G_D^{\mathrm{HF}}(\mathbf{q}) = \frac{2q^{D-3}}{(2\pi)^{2D}n^2}\int_{|\mathbf{s}+\frac{\mathbf{t}}{2}|\leqslant q_F}\int_{|\mathbf{s}-\frac{\mathbf{t}}{2}|\leqslant q_F}\frac{\mathbf{q}\cdot(\mathbf{q}+\mathbf{t})}{|\mathbf{q}+\mathbf{t}|^{D-1}}d\mathbf{t}d\mathbf{s}\,. \tag{B1}$$

Because the integrand only depends on $\mathbf{q}$ and $\mathbf{t}$, we can perform the integration over $\mathbf{s}$. This gives us the volume of the integration region and the integral becomes:

$$G_D^{\mathrm{HF}}(\mathbf{q}) = \frac{2q^{D-3}}{(2\pi)^{2D}n^2}\int d\mathbf{t}\frac{\mathbf{q}\cdot(\mathbf{q}+\mathbf{t})}{|\mathbf{q}+\mathbf{t}|^{D-1}}\int d\mathbf{s}\Theta(q_F-|\mathbf{s}+\tfrac{\mathbf{t}}{2}|)\Theta(q_F-|\mathbf{s}-\tfrac{\mathbf{t}}{2}|)\,. \tag{B2}$$

Thus we need to identify the region in hyperspace in which we are integrating. The region after the substitution is mathematically defined by $|\mathbf{s}+\mathbf{t}/2|\leqslant q_F$ and $|\mathbf{s}-\mathbf{t}/2|\leqslant q_F$ and therefore can be seen as the overlap region of two Fermi spheres in hyperspace (as shown by the colored region in figure 7). The centers of the spheres sit at a distance $|\mathbf{t}|$ from each other, the origin of $\mathbf{s}$ is the midpoint of the connecting line of two centers.

The integration over $\mathbf{s}$ is the volume of this overlap region, which is the combined volumes of two identical hyperspherical caps. The volume of a D-dimensional hyperspherical cap was already calculated by Li [78]:

$$\mathcal{V}_D = \frac{1}{2}V_D(r)\mathrm{I}_{\sin^2\phi}\left(\frac{D+1}{2},\frac{1}{2}\right),$$

where $V_D(r)$ is the volume of a hypersphere with radius r in D-dimensional space, ϕ is the angle between a vector and the positive D^{th}-axis of the sphere and $\mathrm{I}(x,y)$ is the regularized incomplete beta function. In our case it can easily be verified that $\sin^2\phi = 1-\frac{t^2}{4{q_F}^2}$ and $V_D(r) = \pi^{D/2}{q_F}^D/\Gamma\left(\frac{D}{2}+1\right)$. As a result, $G_{\mathrm{HF}}^D(\mathbf{q})$ becomes:

$$G_D^{\mathrm{HF}}(\mathbf{q}) = \frac{2q^{D-3}}{(2\pi)^{2D}n^2}\frac{\pi^{D/2}}{\Gamma\left(\frac{D}{2}+1\right)}{q_F}^D\int \mathrm{I}_{1-\frac{t^2}{4{q_F}^2}}\left(\frac{D+1}{2},\frac{1}{2}\right)\frac{\mathbf{q}\cdot(\mathbf{q}+\mathbf{t})}{|\mathbf{q}+\mathbf{t}|^{D-1}}d\mathbf{t}\,. \tag{B3}$$

By changing to D-dimensional spherical coordinates such that $\mathbf{q}$ is parallel to the D^{th}-axis and using the relation between the density and the Fermi wavelength q_F we obtain equation (16). For some cases this calculation can be done analytically. Here we provide the result for the $5D$ case:

$$\begin{aligned} G_5^{\mathrm{HF}}(q) = {} & \frac{-5}{4928}\left(\frac{q}{q_F}\right)^8 + \frac{25}{1232}\left(\frac{q}{q_F}\right)^6 + \frac{1775}{7392}\left(\frac{q}{q_F}\right)^4 - \frac{5}{66}\left(\frac{q}{q_F}\right)^2 + \frac{25}{154} \\ & + \left[\frac{-15}{128}\left(\frac{q}{q_F}\right)^5 + \frac{15}{224}\left(\frac{q}{q_F}\right)^3 + \frac{5}{56}\left(\frac{q}{q_F}\right) - \frac{25}{154}\left(\frac{q_F}{q}\right)\right]\ln\left|\frac{q+2q_F}{q-2q_F}\right| \qquad \text{(B4)} \\ & + \left[\frac{-5}{19712}\left(\frac{q}{q_F}\right)^{10} + \frac{5}{896}\left(\frac{q}{q_F}\right)^8 - \frac{15}{224}\left(\frac{q}{q_F}\right)^6\right]\ln\left|\frac{q^2-4{q_F}^2}{q^2}\right|. \qquad \text{(B4)} \end{aligned}$$

Appendix C. Compressibility sum rule

By applying the compressibility sum rule (see, for instance, [34]) one can rewrite the dielectric function in the limit $q \to 0$ at $\omega = 0$ as follows:

$$\lim_{q\to 0} \epsilon_D(q,0) = 1 + \Phi(q) n^2 \kappa = 1 + \frac{(4\pi)^{\frac{D-1}{2}} \Gamma\left(\frac{D-1}{2}\right)}{q^{D-1}} \frac{D r_s^2 n}{\alpha_D^2} \frac{\kappa}{\kappa_f}, \tag{C1}$$

where $\kappa_f = \frac{D r_s^2}{n \alpha_D^2}$ is the free compressibility. By defining the D-dimensional Thomas-Fermi wavelength as:

$$q_{\mathrm{TF}} = \left(\frac{(4\pi)^{\frac{D-1}{2}} \Gamma\left(\frac{D-1}{2}\right) D r_s^2 n}{\alpha_D^2} \right)^{\frac{1}{D-1}}$$

we obtain equation (29). In 3D this amounts to the well-known result

$$\lim_{q\to 0} \epsilon_3(\mathbf{q},\omega) = 1 + \frac{q_{\mathrm{TF}}^2}{q^2} \frac{\kappa}{\kappa_f}.$$

Finally, by applying the sum rules to the Lindhard polarizability (i.e. $\lim_{q\to 0} \chi_0(q,0) = -n^2 \kappa_f$,) we obtain the dielectric function in the STLS theory (equation (8)) in the limit $q \to 0$:

$$\lim_{q\to 0} \epsilon_D(\mathbf{q},0) = 1 + \frac{\left(\frac{q_{\mathrm{TF}}}{q}\right)^{D-1}}{1 - \gamma_D \left(\frac{q_{\mathrm{TF}}}{q_F}\right)^{D-1}}, \tag{C2}$$

where $\gamma_D = -\frac{1}{2q_F} \int_0^\infty [S_D(q) - 1] dq$. From equation (29) one eventually finds:

$$\frac{\kappa_f}{\kappa} = 1 - \gamma_D \left(\frac{q_{\mathrm{TF}}}{q_F}\right)^{D-1}. \tag{C3}$$

ORCID iDs

L V Duc Pham https://orcid.org/0000-0001-7166-593X
Miguel A L Marques https://orcid.org/0000-0003-0170-8222
Carlos L Benavides-Riveros https://orcid.org/0000-0001-6924-727X

References

[1] Landau L D, Lifshitz E M and Pitaevskii L P 1980 *Statistical Physics: Theory of the Condensed State* (*Course of Theoretical Physics*) (Elsevier Science)
[2] Migdal A B 1967 *Theory of Finite Fermi Systems and Application to Atomic Nuclei* (Wiley-Interscience Publ.)
[3] Sommerfeld A 1928 Zur elektronentheorie der metalle auf grund der fermischen statistik *Z. Phys.* **47** 1
[4] Rajagopal A K and Kimball J C 1977 Correlations in a two-dimensional electron system *Phys. Rev.* B **15** 2819
[5] Gori-Giorgi P and Ziesche P 2002 Momentum distribution of the uniform electron gas: improved parametrization and exact limits of the cumulant expansion *Phys. Rev.* B **66** 235116
[6] Huotari S *et al* 2010 Momentum distribution and renormalization factor in sodium and the electron gas *Phys. Rev. Lett.* **105** 086403
[7] Holzmann M, Bernu B, Pierleoni C, McMinis J, Ceperley D M, Olevano V and Delle Site L 2011 Momentum distribution of the homogeneous electron gas *Phys. Rev. Lett.* **107** 110402
[8] Shepherd J J, Booth G, Grüneis A and Alavi A 2012 Full configuration interaction perspective on the homogeneous electron gas *Phys. Rev.* B **85** 081103(R)
[9] Lewin M, Lieb E H and Seiringer R 2018 Statistical mechanics of the uniform electron gas *J. Éc. Polytech. - Math.* **5** 79
[10] Loos P-F and Gill P M W 2016 The uniform electron gas *WIREs Comput. Mol. Sci.* **6** 410
[11] Zhang S and Ceperley D M 2008 Hartree-Fock ground state of the three-dimensional electron gas *Phys. Rev. Lett.* **100** 236404
[12] Gontier D, Hainzl C and Lewin M 2019 Lower bound on the Hartree-Fock energy of the electron gas *Phys. Rev.* A **99** 052501
[13] Drummond N D and Needs R J 2009 Phase diagram of the low-density two-dimensional homogeneous electron gas *Phys. Rev. Lett.* **102** 126402
[14] Spink G G, Needs R J and Drummond N D 2013 Quantum Monte Carlo study of the three-dimensional spin-polarized homogeneous electron gas *Phys. Rev.* B **88** 085121
[15] Ma S-K and Brueckner K A 1968 Correlation energy of an electron gas with a slowly varying high density *Phys. Rev.* **165** 18
[16] Ceperley D M and Alder B J 1980 Ground state of the electron gas by a stochastic method *Phys. Rev. Lett.* **45** 566
[17] Jones R O 2015 Density functional theory: its origins, rise to prominence and future *Rev. Mod. Phys.* **87** 897
[18] Constantin L A, Pitarke J M, Dobson J F, Garcia-Lekue A and Perdew J P 2008 High-level correlated approach to the jellium surface energy, without uniform-gas input *Phys. Rev. Lett.* **100** 036401

[19] Wagner L O, Stoudenmire E M, Burke K and White S R 2012 Reference electronic structure calculations in one dimension *Phys. Chem. Chem. Phys.* **14** 8581
[20] Astrakharchik G E, Krutitsky K V, Lewenstein M and Mazzanti F 2016 One-dimensional Bose gas in optical lattices of arbitrary strength *Phys. Rev.* A **93** 021605(R)
[21] Schmidt J, Benavides-Riveros C L and Marques M A L 2019 Machine learning the physical nonlocal exchange-correlation functional of density-functional theory *J. Phys. Chem. Lett.* **10** 6425
[22] Constantin L A 2016 Simple effective interaction for dimensional crossover *Phys. Rev.* B **93** 121104(R)
[23] Gedeon J, Schmidt J, Hodgson M J P, Wetherell J, Benavides-Riveros C L and Marques M A L 2022 Machine learning the derivative discontinuity of density-functional theory *Mach. Learn.: Sci. Technol.* **3** 015011
[24] Kwon Y, Ceperley D M and Martin R M 1994 Quantum Monte Carlo calculation of the Fermi-liquid parameters in the two-dimensional electron gas *Phys. Rev.* B **50** 1684
[25] Voit J 1995 One-dimensional Fermi liquids *Rep. Progr. Phys.* **58** 977
[26] Kennes D M, Claassen M, Xian L, Georges A, Millis A J, Hone J, Dean C R, Basov D N, Pasupathy A N and Rubio A 2021 Moiré heterostructures as a condensed-matter quantum simulator *Nat. Phys.* **17** 155
[27] Kempkes S N, Slot M R, Freeney S E, Zevenhuizen S J M, Vanmaekelbergh D, Swart I and Smith C M 2019 Design and characterization of electrons in a fractal geometry *Nat. Phys.* **15** 127
[28] van Veen E, Yuan S, Katsnelson M I, Polini M and Tomadin A 2016 Quantum transport in Sierpinski carpets *Phys. Rev.* B **93** 115428
[29] Fremling M, van Hooft M, Smith C M and Fritz L 2020 Existence of robust edge currents in Sierpiński fractals *Phys. Rev. Res.* **2** 013044
[30] Hummel F, Eiles M T and Schmelcher P 2021 Synthetic dimension-induced conical intersections in Rydberg molecules *Phys. Rev. Lett.* **127** 023003
[31] Kanungo S K, Whalen J D, Lu Y, Yuan M, Dasgupta S, Dunning F B, Hazzard K R A and Killian T C 2022 Realizing topological edge states with Rydberg-atom synthetic dimensions *Nat. Commun.* **13** 972
[32] Ghosh S K, Greschner S, Yadav U K, Mishra T, Rizzi M and Shenoy V B 2017 Unconventional phases of attractive Fermi gases in synthetic Hall ribbons *Phys. Rev.* A **95** 063612
[33] Celi A, Massignan P, Ruseckas J, Goldman N, Spielman I B, Juzeliūnas G and Lewenstein M 2014 Synthetic gauge fields in synthetic dimensions *Phys. Rev. Lett.* **112** 043001
[34] Giuliani G and Vignale G 2005 *Quantum Theory of the Electron Liquid* (Cambridge University Press)
[35] Schlesier R, Benavides-Riveros C L and Marques M A L 2020 Homogeneous electron gas in arbitrary dimensions *Phys. Rev.* B **102** 035123
[36] Ren X, Rinke P, Joas C and Scheffler M 2012 Random-phase approximation and its applications in computational chemistry and materials science *J. Mater. Sci.* **47** 7447
[37] Gubernatis J, Kawashima N and Werner P 2016 *Quantum Monte Carlo Methods: Algorithms for Lattice Models* (Cambridge University Press)
[38] Singwi K S, Tosi M P, Land R H and Sjölander A 1968 Electron correlations at metallic densities *Phys. Rev.* **176** 589
[39] Agosti D, Pederiva F, Lipparini E and Takayanagi K 1998 Ground-state properties and density response of quasi-one-dimensional electron systems *Phys. Rev.* B **57** 14869
[40] Dobson J F 2009 Inhomogeneous STLS theory and TDCDFT *Phys. Chem. Chem. Phys.* **11** 4528
[41] Kosugi T and Matsushita Y 2017 Quantum Singwi-Tosi-Land-Sjölander approach for interacting inhomogeneous systems under electromagnetic fields: comparison with exact results *J. Chem. Phys.* **147** 114105
[42] Dharma-wardana M W C 1981 The dynamic response of a non-uniform distribution of electrons *J. Phys. C: Solid State Phys.* **14** L167
[43] Tanaka S 2017 Improved equation of state for finite-temperature spin-polarized electron liquids on the basis of Singwi-Tosi-Land-Sjölander approximation *Contrib. Plasma Phys.* **57** 126
[44] Dornheim T, Vorberger J, Moldabekov Z A and Tolias P 2022 Spin-resolved density response of the warm dense electron gas *Phys. Rev. Res.* **4** 033018
[45] Dornheim T, Groth S and Bonitz M 2018 The uniform electron gas at warm dense matter conditions *Phys. Rep.* **744** 1
[46] Dobson J F, Wang J and Gould T 2002 Correlation energies of inhomogeneous many-electron systems *Phys. Rev.* B **66** 081108(R)
[47] Vilk Y M, Chen L and Tremblay A-M S 1994 Theory of spin and charge fluctuations in the Hubbard model *Phys. Rev.* B **49** 13267
[48] Zantout K, Backes S and Valentí R 2021 Two-particle self-consistent method for the multi-orbital Hubbard model *Ann. Phys.* **533** 2000399
[49] Yoshizawa K and Takada Y 2009 New general scheme for improving accuracy in implementing self-consistent iterative calculations: illustration in the STLS theory *J. Phys.: Condens. Matter* **21** 064204
[50] Hasegawa T and Shimizu M 1975 Electron correlations at metallic densities, II. Quantum mechanical expression of dielectric function with Wigner distribution function *J. Phys. Soc. Japan* **38** 965
[51] Zhang S-C and Hu J 2001 A four-dimensional generalization of the quantum Hall effect *Science* **294** 823
[52] Lohse M, Schweizer C, Price H M, Zilberberg O and Bloch I 2018 Exploring 4D quantum Hall physics with a 2D topological charge pump *Nature* **553** 55
[53] Dutt A, Minkov M, Lin Q, Yuan L, Miller D A B and Fan S 2019 Experimental band structure spectroscopy along a synthetic dimension *Nat. Commun.* **10** 3122
[54] Chen Y-A 2020 Exact bosonization in arbitrary dimensions *Phys. Rev. Res.* **2** 033527
[55] Boada O, Celi A, Latorre J I and Lewenstein M 2012 Quantum simulation of an extra dimension *Phys. Rev. Lett.* **108** 133001
[56] Pines D 1999 *Elementary Excitations in Solids* (CRC Press)
[57] Pines D and Noziéres P 1966 *The Theory of Quantum Liquids: Normal Fermi Liquids* (CRC Press)
[58] Bernadotte S, Evers F and Jacob C R 2013 Plasmons in molecules *J. Phys. Chem.* C **117** 1863
[59] Vashishta P and Singwi K S 1972 Electron correlations at metallic densities. V *Phys. Rev.* B **6** 875–87
[60] Sham L J 1973 Exchange and correlation in the electron gas *Phys. Rev.* B **7** 4357
[61] Haug H and Koch S W 2009 *Quantum Theory of the Optical and Electronic Properties of Semiconductors* 5th edn (World Scientific Publishing Co.)
[62] Ferrell R A 1958 Rigorous validity criterion for testing approximations to the electron gas correlation energy *Phys. Rev. Lett.* **1** 443
[63] Kumar K, Garg V and Moudgil R K 2009 Spin-resolved correlations and ground state of a three-dimensional electron gas: spin-polarization effects *Phys. Rev.* B **79** 115304
[64] Ng T K and Singwi K S 1987 Arbitrarily polarized model Fermi liquid *Phys. Rev.* B **35** 6683

[65] Ceperley D 1978 Ground state of the fermion one-component plasma: a monte carlo study in two and three dimensions *Phys. Rev.* B **18** 3126
[66] Monnier R 1972 Monte Carlo approach to the correlation energy of the electron gas *Phys. Rev.* A **6** 393
[67] Jonson M 1976 Electron correlations in inversion layers *J. Phys. C: Solid State Phys.* **9** 3055
[68] We corrected a small error in the numerical evaluation of the coefficients presented in table 1 of [35] that however does not affect the main conclusions of that paper.
[69] Sjostrom T and Dufty J 2013 Uniform electron gas at finite temperatures *Phys. Rev.* B **88** 115123
[70] Vaishya J S and Gupta A K 1973 Dielectric Response of the electron liquid in generalized random-phase approximation: a critical analysis *Phys. Rev.* B **7** 4300
[71] Pai S and Prem A 2019 Topological states on fractal lattices *Phys. Rev.* B **100** 155135
[72] Pal B and Saha K 2018 Flat bands in fractal-like geometry *Phys. Rev.* B **97** 195101
[73] Brzezińfiska M, Cook A M and Neupert T 2018 Topology in the Sierpiński-Hofstadter problem *Phys. Rev.* B **98** 205116
[74] Benavides-Riveros C L, Lathiotakis N N and Marques M A L 2017 Towards a formal definition of static and dynamic electronic correlations *Phys. Chem. Chem. Phys.* **19** 12655
[75] Lewin M 2022 Coulomb and Riesz gases: the known and the unknown *J. Math. Phys.* **63** 061101
[76] Bonitz M, Dornheim T, Moldabekov Z A, Zhang S, Hamann P, Kählert H, Filinov A, Ramakrishna K and Vorberger J 2020 *Ab initio* simulation of warm dense matter *Phys. Plasmas* **27** 042710
[77] Singwi K S and Tosi M P 1981 Correlations in electron liquids *Solid State Phys.* **36** 177
[78] Li S 2011 Concise formulas for the area and volume of a hyperspherical cap *Asian J. Math. Stat.* **4** 66